



## Development of a prototype 6 degree of freedom robot arm

Tran Thanh Tung<sup>a</sup>, Nguyen Van Tinh<sup>b</sup>, Dinh Thi Phuong Thao<sup>b</sup>, Tran Vu Minh<sup>b,\*</sup>

<sup>a</sup> Faculty of Engineering Mechanics and Automation, University of Engineering and Technology, Vietnam National University, Hanoi, Viet Nam

<sup>b</sup> School of Mechanical Engineering, Ha Noi University of Science and Technology, Ha Noi, Viet Nam

### ARTICLE INFO

#### Keywords:

Robot arm  
AR3  
6 DOF  
Topology optimization  
Kinematics

### ABSTRACT

The study presents a design alternative, simulates the operation, and analyzes the new structure of the 6 DOF robot arm. The proposed robot model is based on reference shapes from AR3 robot arm, with modifications to details and structures to accommodate the actual and economic circumstances in Vietnam. Solidwork software was first utilized for the arm structure's design, strength testing, and optimization. The material is chosen with the goal of reducing production cost and ensuring the robot's operation properly. The study concludes by applying the topology optimization algorithm to a machine component to determine the optimal structure of the robot arm. To validating the design results, the prototype is manufactured using CNC machine. The experimental results show the robot arm basic functions effectively. This research could be used as references for designing and manufacturing a 6 DOF robot arm with relative robot's structure.

### 1. Introduction

Robot is no longer a foreign concept to modern society [1–5]. They are gradually being viewed by the technical community as specialized machines, adapted by humans according to their own structure and operation, that can replace humans in a number of occupations [6–9]. Typically, an Industrial Robot can be viewed as a universal device that is automated based on a program and can be reprogrammed to respond flexibly and competently to various factory tasks. Typical industrial applications for these robots include transporting and unloading materials, assembling, measuring, etc. Currently, the demand for industrial robots is on the rise, and the types of robots manufactured are becoming increasingly diverse, with higher precision, greater adaptability, more affordable prices, greater productivity, and a longer lifespan [10–14].

The industrial robotic arm is one of the most frequently employed robots in manufacturing. In the majority of cases, they are programmed and used to carry out specific tasks, generally in manufacturing, fabrication, and heavy industrial applications [15–19]. The industrial robot arm functions similarly to a human arm [20–23]. With a flexible knuckle mechanism, the finger can travel along the axis or rotate in particular directions. Due to these exceptional benefits, these mechanical machines are being utilized in a variety of areas, including plastic production. In manufacturing, robotic arms have replaced human hands. Assembling, repairing, and replacing micro-components in the factory, as well as loading and unloading goods according to their assigned placements, are

some of the production line tasks that robotic arms are designed to execute. Available. In addition, the Robotic Arm can aid with product quality inspection [24–28].

The action mechanism of a robot arm is dependent on the connection between the controller and the motion joints. Therefore, the active control unit issues commands to the arm's joints so that it can translate (linear) or rotate (as in an articulated robot). These links are fitted in accordance with production specifications to form a kinematic chain. The completion of this chain of events is referred to as the end effect, and its operating rules imitate the action of a human hand flawlessly [29–33].

The purpose of this study is to propose a mechanical design and manufacturing process for a 6-degrees-of-freedom robotic arm with the goal of lower cost than comparable goods but still fully functional. The structure of this paper as follow, the article presents the preliminary structure of the robot arm, and Section 2 introduces the kinematic problems. The third and fourth sections of the article discuss the evaluation of stability and optimizing the structure of the robot arm. A prototype is manufactured and discussed in Section 5, and finally, Section 6 concludes this paper.

\* Corresponding author.

E-mail address: [minh.tranvu@hust.edu.vn](mailto:minh.tranvu@hust.edu.vn) (T.V. Minh).

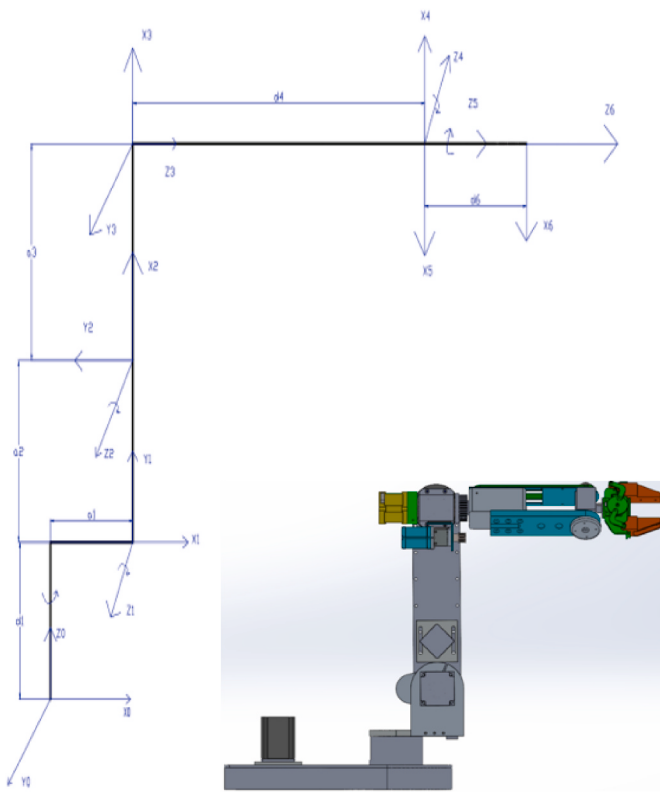


**Fig. 1.** Kinematic diagram coordinate axes at the joints of the robot.

**Table 1**  
Denavit Hartenberg table of kinematic parameters of the robot.

Joints	$\theta_i$	$d_i$	$a_i$	$\alpha_i$
1	$\theta_1$	$d_1$	$a_1$	- 90°
2	$\theta_2$	0	$a_2$	0
3	$\theta_3$	0	0	90°
4	$\theta_4$	$d_4$	0	90°
5	$\theta_5$	$d_5$	0	90°
6	$\theta_6$	$d_6$	0	0

**Table 2**  
Joint angle.

Angle	Value
$\theta_1$	$\theta_1 = ATAN 2(\pm(-a_y d_6 + p_y), \pm(-a_x d_6 + p_x))$
$\theta_2$	$\theta_2 = ATAN 2(ad - bc, ac + bd)$
$\theta_3$	$\theta_3 = ATAN' 2(X, \pm\sqrt{1 - X^2})$
$\theta_4$	$\theta_4 = ATAN 2(s_4, c_4)$
$\theta_5$	$\theta_5 = ATAN 2(\pm\sqrt{1 - k_1^2}, k_1)$
$\theta_6$	$\theta_6 = ATAN 2(s_6, c_6)$

**Table 3**  
Static parameters.

Parameter	Value
m1	3 kg
m2	2.5 kg
m3	1 kg
m4	2 kg
m5	0.7 kg
m6	0.5 kg



**Fig. 2.** The position of the robot arm's rotation joint.

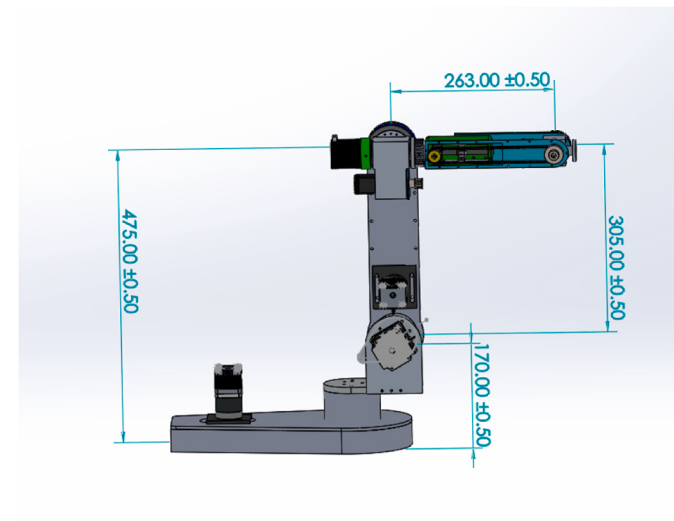


**Fig. 3.** Overview of the robot arm.

**Table 4**  
Material properties.

Property	Value	Units
Elastic Modulus	69000	N/mm <sup>2</sup>
Poisson's Ratio	0.33	N/A
Shear Modulus	26000	N/mm <sup>2</sup>
Mass Density	2700	kg/m <sup>3</sup>
Tensile Strength	310	N/mm <sup>2</sup>
Yield Strength	55	Mpa

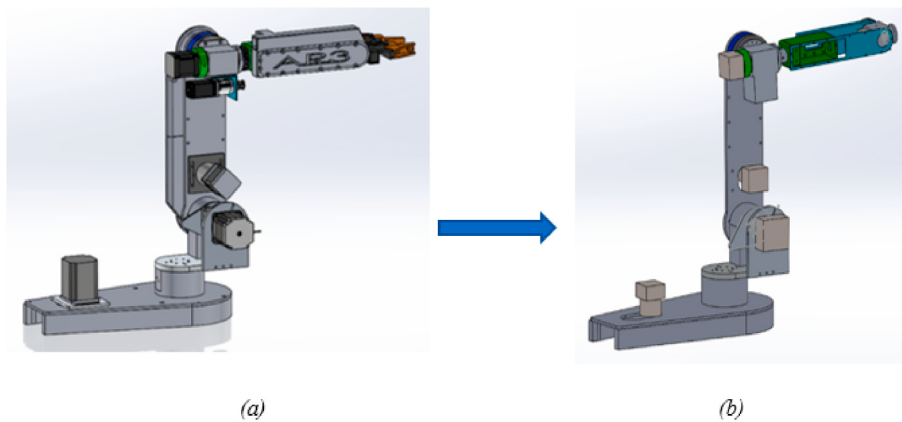


**Fig. 4.** Model before (a) and (b) after simplification.

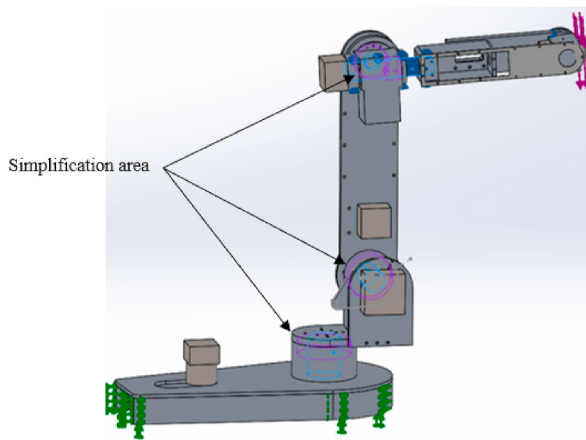


**Fig. 5.** Virtual link points.

## 2. Methodology

### 2.1. Design objective

The objective of this project is to built a robotic arm with 6 DOF that has working dimension is similar as a human arm and can grasp an object along a predetermined trajectory. The robot arm can reach a maximum distance of 550 mm and a maximum height of 720 mm. The robotic arm has the ability to grasp things weighing up to 0.5 kg. Structure diagram of proposed robot arm as shown in the Fig. 1 where:

$x_i, y_i, z_i$  are coordinates of each joint.

$d_i$  is the offset from along  $z_{i-1}$  to the common normal.

$\theta_i$  is angle about  $z_{i-1}$ , from old x axis to new x axis.

$a_i$  is the length of common normal.

$\alpha_i$  is angle about common normal, from old z axis to new z axis.

### 2.2. Kinematic analysis

Based on the proposed construction, Table 1 displays the DH parameters of the robot arm.

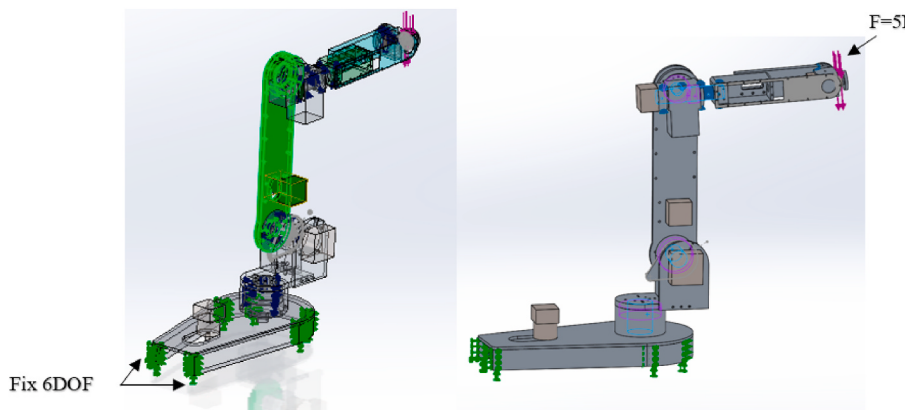
Using the parameters from Table 1, the following forward kinematic equation can be generated to determine the transformation matrix of the connecting rod:

$${}^0A^a_1 = \begin{bmatrix} \cos \theta_1 & 0 & -\sin \theta_1 & a_1 \cos \theta_1 \\ \sin \theta_1 & 0 & \cos \theta_1 & a_1 \sin \theta_1 \\ 0 & -1 & 0 & d_1 \\ 0 & 0 & 0 & 1 \end{bmatrix}, {}^1A^1_2 = \begin{bmatrix} \cos \theta_2 & -\sin \theta_2 & 0 & a_2 \cdot \cos \theta_2 \\ \sin \theta_2 & \cos \theta_2 & 0 & a_2 \cdot \sin \theta_2 \\ 0 & 0 & 1 & 0 \\ 0 & 0 & 0 & 1 \end{bmatrix}$$

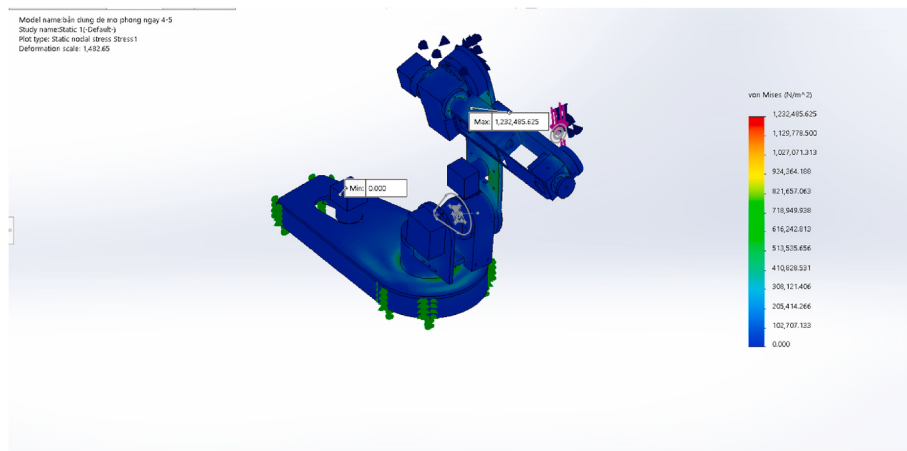
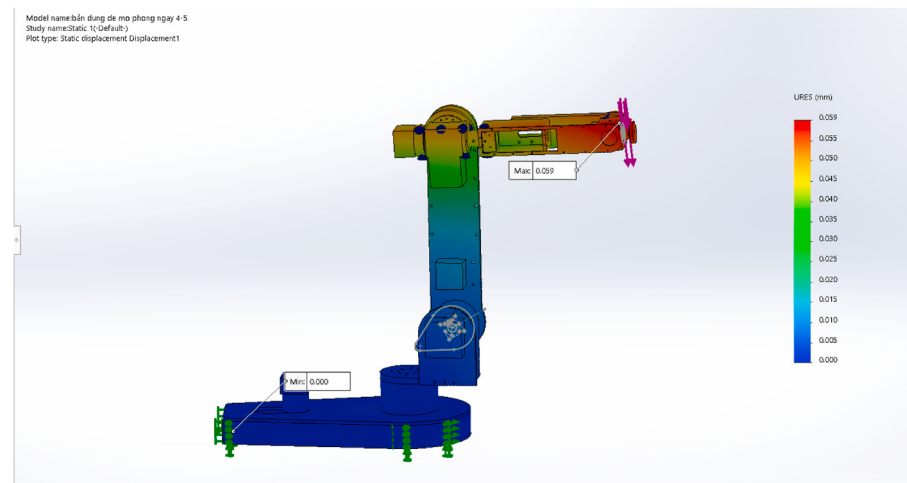
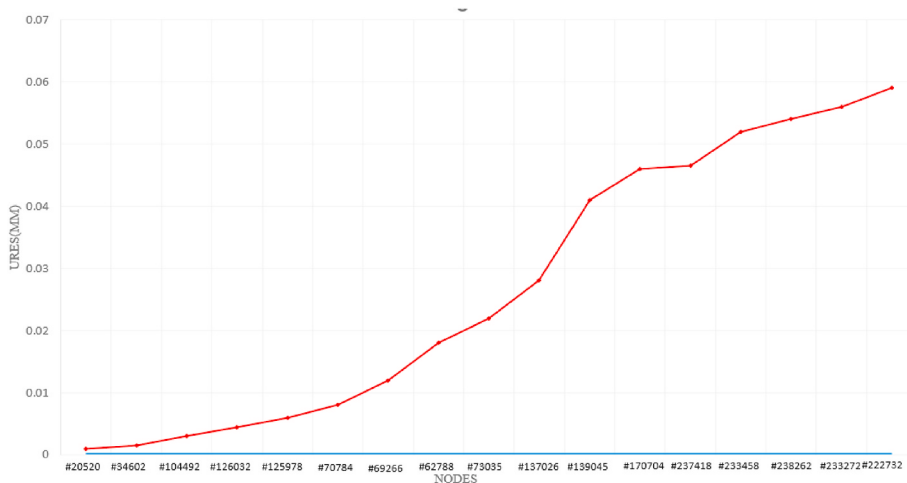
$${}^1A^1_3 = \begin{bmatrix} \cos \theta_3 & 0 & \sin \theta_3 & 0 \\ \sin \theta_3 & 0 & -\cos \theta_3 & 0 \\ 0 & 1 & 0 & 0 \\ 0 & 0 & 0 & 1 \end{bmatrix}, {}^3A^1_4 = \begin{bmatrix} \cos \theta_4 & 0 & \sin \theta_4 & 0 \\ \sin \theta_4 & 0 & -\cos \theta_4 & 0 \\ 0 & 1 & 0 & d_4 \\ 0 & 0 & 0 & 1 \end{bmatrix}$$

$${}^4A^1_5 = \begin{bmatrix} \cos \theta_5 & 0 & \sin \theta_5 & 0 \\ \sin \theta_5 & 0 & -\cos \theta_5 & 0 \\ 0 & 1 & 0 & 0 \\ 0 & 0 & 0 & 1 \end{bmatrix}, {}^5A^1_6 = \begin{bmatrix} \cos \theta_6 & -\sin \theta_6 & 0 & 0 \\ \sin \theta_6 & \cos \theta_6 & 0 & 0 \\ 0 & 0 & 1 & d_6 \\ 0 & 0 & 0 & 1 \end{bmatrix}$$

The end matrix is as follow :  ${}^0A^1_6 = {}^0A^1_1 \cdot {}^1A^1_2 \cdot {}^2A^1_3 \cdot {}^3A^1_4 \cdot {}^4A^1_5 \cdot {}^5A^1_6$  (1)



**Fig. 6.** Boundary condition.

**Fig. 7.** Stress simulation results.**Fig. 8.** Displacement simulation results.**Fig. 9.** Displacement value from base to final link.

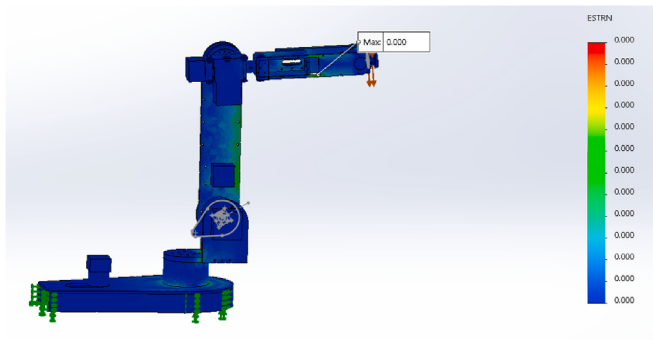


Fig. 10. Simulation results of deformation.

The direction and position of the wrist are represented with respect to the external fixed coordinate system ((world coordinate system  $O_0$ ). We have to solve the above problem for the unknowns  $\theta_1, \dots, \theta_6$ . The sixth structure rotation joints with the last 3 joints intersect with the solution method as follows: The position of the wrist center  $R_c$  is determined through the tool position (The given tool position - relative to the coordinate system  $O_0$ ) and the direction of the Tool pointing ( $Z_6$ .) Because the position of the center of the wrist depends on the first 3 joint variables.

Joint variables  $\theta_4, \theta_5, \theta_6$  determined from the given tool orientation matrix  ${}^3T_6^1$  ( $\theta_1, \theta_2, \theta_3$ ) and matrix.

$${}^3T_6^1 = {}^3T_3^{0^{-1}}(\theta_1, \theta_2, \theta_3) * {}_1T_6^1 \quad (2)$$

where  ${}^3T_3^{0^{-1}}$  is the arm orientation matrix from previous link.

For the inverse kinematic problem, Table 2 describes the position of the robot arm's link when the position of the end link was known for the inverse problem. The result of the angles  $\theta_1, \theta_2, \theta_3, \theta_4, \theta_5, \theta_6$  were as follows

### 2.3. Static analysis

Robotic static force analysis is essential for calculating the value of the force transmitted through the mechanism's joints. This result will serve as the foundation for the design and selection of the appropriate link size and drive motors.

Aluminum (6061 Alloy) was chosen as the material for the design based on the SolidWorks databases, and the weight of the links is calculated as shown in the Table 3:

Calculating the driving force (torque) at the joints guarantees the static equilibrium of the robot. The system of balanced equations in the coordinate system of the origin:

$$\left\{ \begin{array}{l} \vec{F}_{i,i-1} = {}^0\vec{F}_{i+1,i} - {}^0\vec{P}_i \\ {}^0\vec{M}_{i,i-1} = {}^0\vec{M}_{i+1,i} - {}^0\vec{r}_i \times {}^0\vec{F}_{i,i-1} - {}^0\vec{r}_{C_i} \times {}^0\vec{P}_i \end{array} \right. \quad (3)$$

in which:

$\vec{F}_{i,i-1}$  in the basic coordinate system, is the force exerted by link i-1 on link i at joint i.

$\vec{M}_{i,i-1}$  is the force that link i-1 exerts on link i at joint i in the basic coordinate system..

${}^0\vec{P}_i$  weight of link i in the fundamental coordinate system

${}^0\vec{r}_i$  is a vector whose origin is  $O_0$  connected to  $O_i$  in the basic coordinate system.

${}^0R_i^1$  is the rotation matrix that transforms from coordinate system 0 to coordinate system i.

${}^i\vec{r}_i$  is a vector whose origin is  $O_{i-1}$  connected to  $O_i$  in the basic coordinate system i

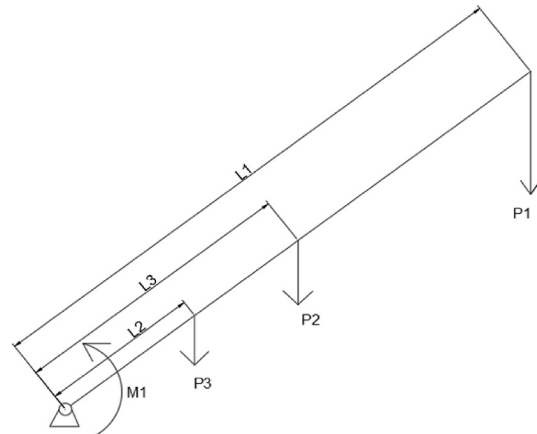


Fig. 12. Force diagram of joint 2 arm.

Table 5  
Parameters in the model.

Parameter	Value	Link	Value (mm)
P1	29.4 (N)	L1	305
P2	2.06(N)	L2	152.5
P3	5.488 (N)	L3	78
M1	51 (Nm)	-	-

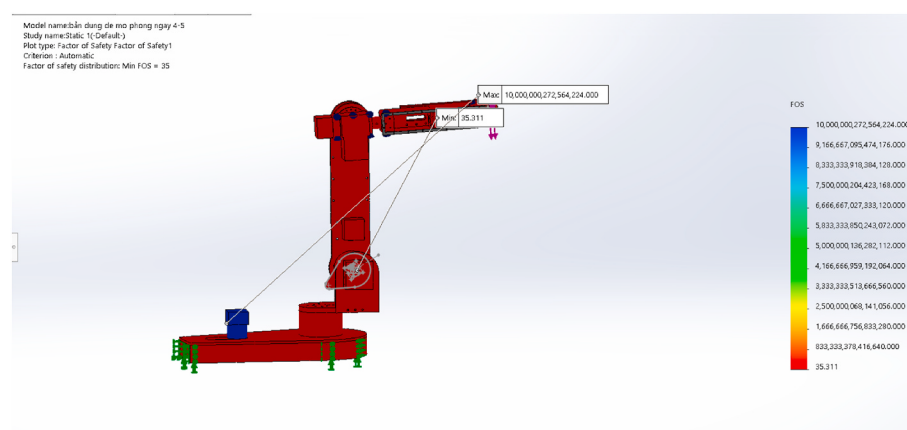


Fig. 11. Factor of safety.

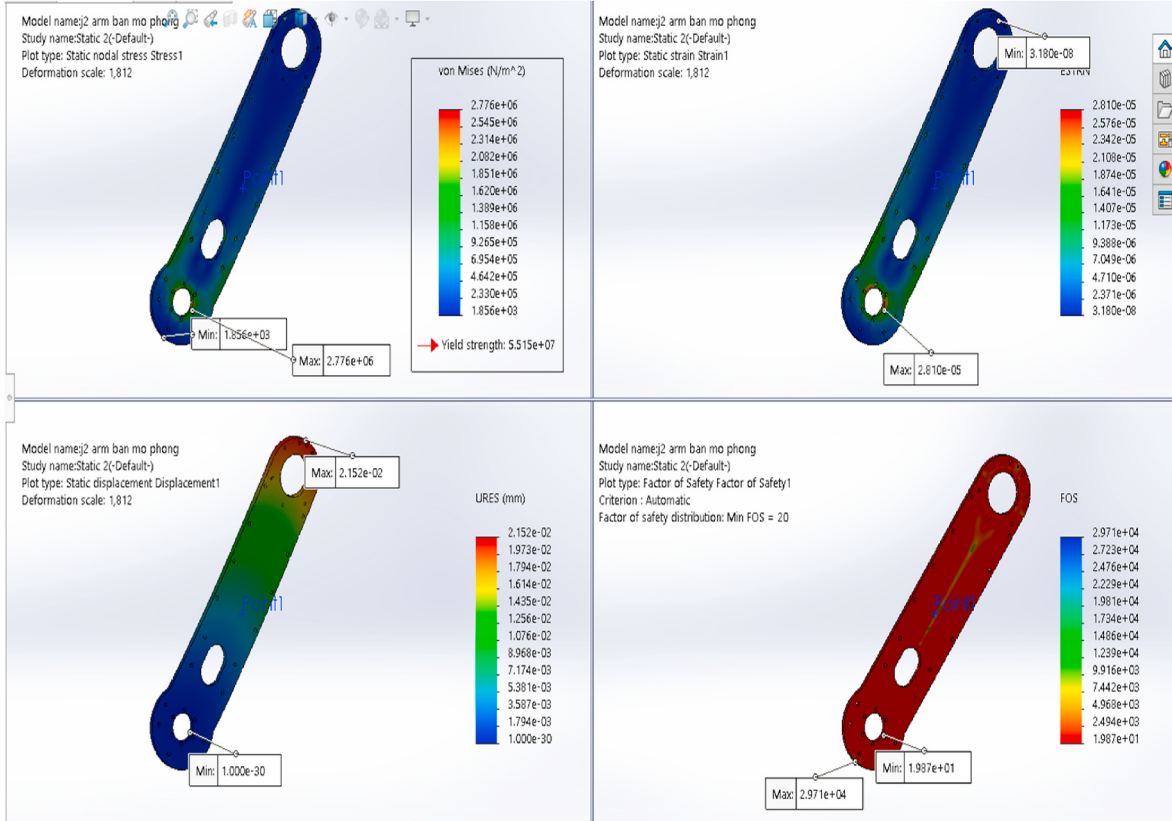


Fig. 13. Results of a JOINT 2 Arm simulation without doing an optimization.

Suppose force in the end-link:

$$F_{E,6} = \begin{bmatrix} 0 \\ 0 \\ 0 \end{bmatrix}, M_{E,6} = \begin{bmatrix} 0 \\ 0 \\ 0 \end{bmatrix} \quad (4)$$

Substituting in the above two equations, we get:  $F_{6,5} = \begin{bmatrix} 0 \\ 0 \\ 49 \end{bmatrix}$ ,

$$M_{dc6} = 0.38 \text{ (N.m)}$$

Calculating similarly for the remaining joints, the following results are obtained::

Static force of each link

$$F_{6,5} = \begin{bmatrix} 0 \\ 0 \\ 49 \end{bmatrix}, F_{5,4} = \begin{bmatrix} 0 \\ 0 \\ 117 \end{bmatrix}, F_{4,3} = \begin{bmatrix} 0 \\ 0 \\ 190 \end{bmatrix}, F_{3,2} = \begin{bmatrix} 0 \\ 0 \\ 289 \end{bmatrix}, F_{2,1} = \begin{bmatrix} 0 \\ 0 \\ 480 \end{bmatrix},$$

$$F_{1,0} = \begin{bmatrix} 0 \\ 0 \\ 779 \end{bmatrix} \quad (5)$$

Torque static of the motor necessary for the balance of robot  
In which:

$$d_1 = 170\text{mm}, a_1 = 70\text{mm}, a_2 = 305\text{mm}, d_4 = 263\text{mm}, d_6 = 60\text{mm}$$

and computed as:

$$M_{dc1} = 0 \text{ (N.m)} M_{dc4} = 1.2 \text{ (N.m)}$$

$$M_{dc2} = 50 \text{ (N.m)} M_{dc5} = 0.4 \text{ (N.m)}$$

$$M_{dc3} = 2.84 \text{ (N.m)} M_{dc6} = 0.38 \text{ (N.m)}$$

### 3. Modeling

#### 3.1. 3D modeling

The robot arm is based on the concept of the previously existing AR3 robot arm [34]. However, this new arm product's structure differs from the AR3's original design in order to accommodate manufacturing capabilities and production conditions. The working function still satisfies the requirements, and the cost reduction relative to the original AR3 design is substantial.

The rotation joints of the 6-step robot arm are depicted in Fig. 2, from left to right and top to bottom, respectively. Fig. 3 depicts the overall structure and dimension of proposed robot arm which is modeled on Solidworks 2018.

#### 3.2. Material selection

For the purpose is low-cost design, Aluminum 6061 alloy is selected as the manufacturing material. The material properties as expressed in Table 4 as follow:

### 4. Stress analysis and topology optimization

#### 4.1. Boundary condition

Fig. 4 depicts how the robot arm has been simplified to assist simulation without significantly affecting the results. The assembly areas are replaced with constraints that limit the freedom of movement.

Installation position of connections between components such as screws, bolts, and so on. At these areas, we will replace physical components such as screws, bolts, and nuts with virtual links as shown in the Fig. 5.

If each screw is positioned in its own mounting location to form a

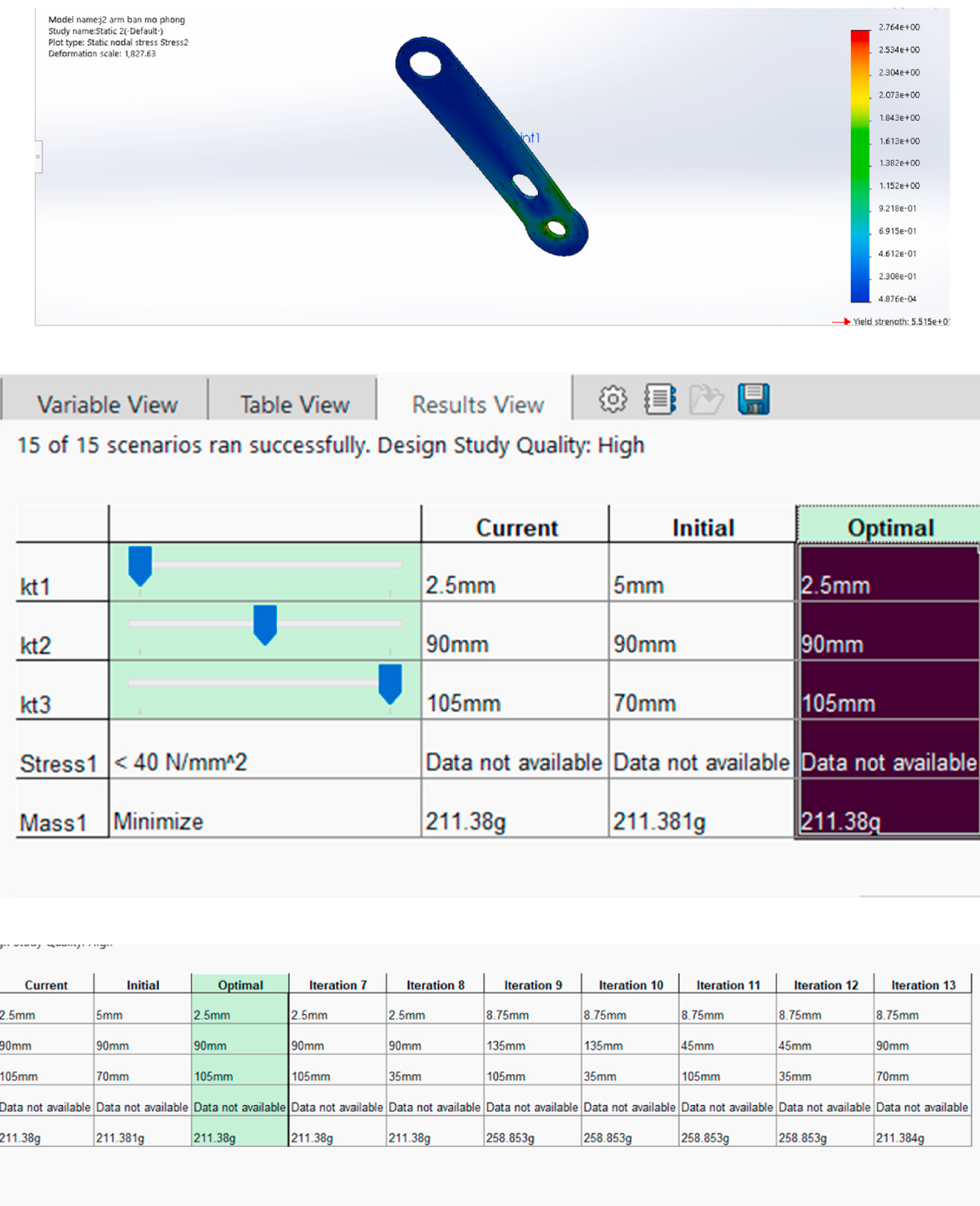


**Fig. 14.** The results from the new structure.

connection between the details, force must be applied to each screw simultaneously. The base of the robot arm has constrained six degrees of freedom, while the connections between the links will have one degree of freedom for translation or rotation, depending on their position. A 5 N load is positioned on the gripper's top. Like an illustration, a boundary condition as seen in the Fig. 6.

#### 4.2. Simulation results

##### 4.2.1. Stress

According to the simulation results (Fig. 7), stress is focused at the points of connection between the details and the big load-bearing

features. The position of the connecting axis with all links 5 and 6 has a maximum stress of 1232 N/mm<sup>2</sup>. Thus, the model can withstand the imposed loads and other environmental restrictions.

##### 4.2.2. Displacement

Fig. 8 show the displacement simulation results, the highest displacement at the position depicted in the image is 0.059 mm, while the minimum displacement at the base position is 0 mm. The degree of displacement of the model when a 5 N force is applied can be seen to be relatively minimal.

As illustrated in the Fig. 9 below, the degree of displacement tends to grow from initial to final actuation.

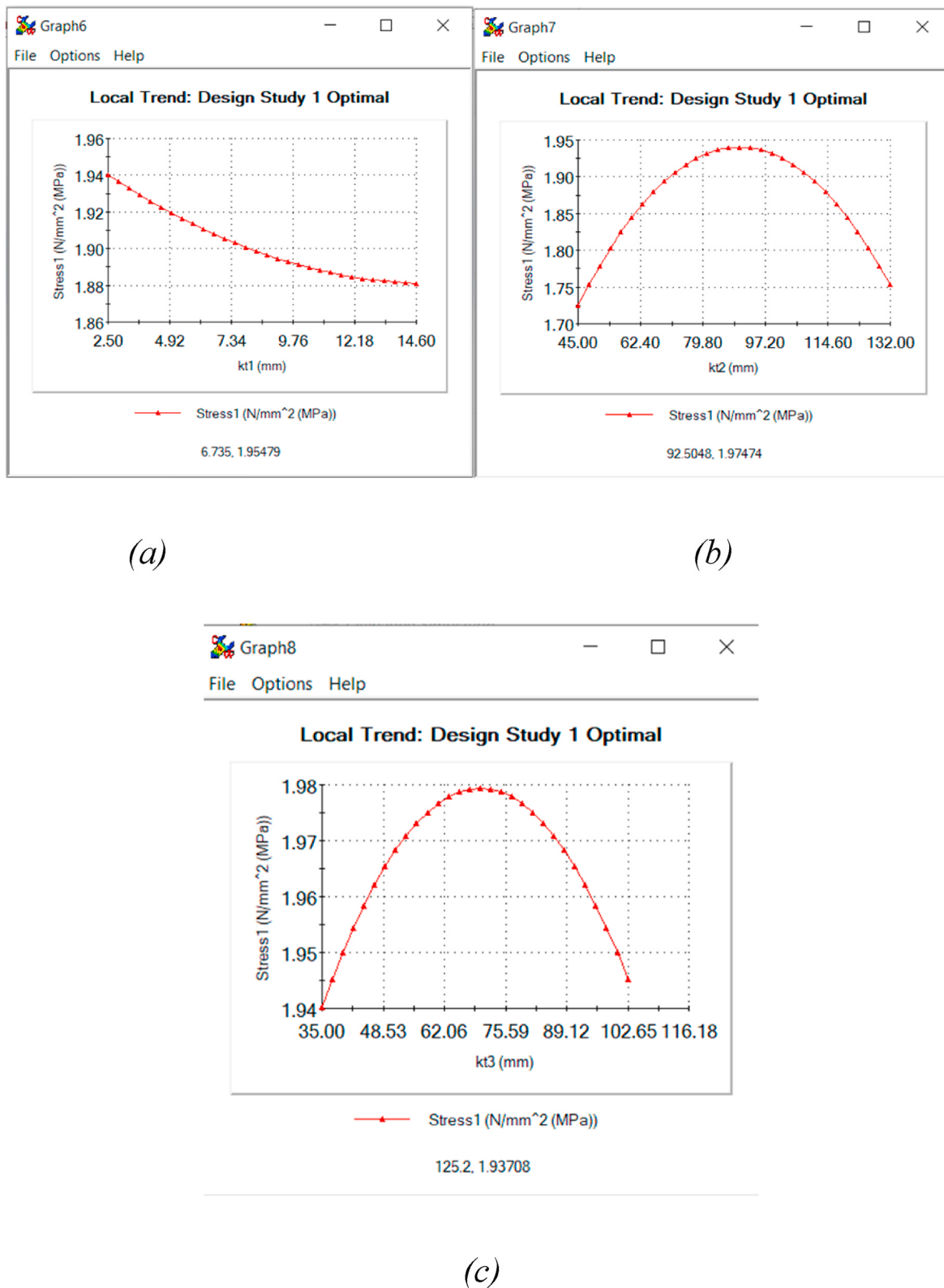
**Fig. 15.** Stress diagram.



Fig. 16. The optimization structure.

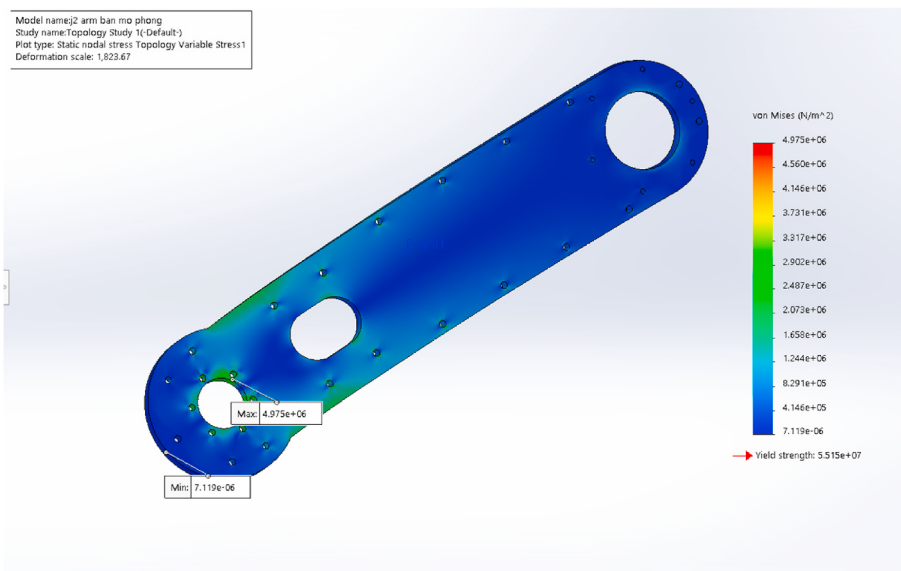


Fig. 17. Stress simulation results from new structure.

#### 4.2.3. Strain

The results of the deformation simulation allow us to determine the location of the greatest deformation, as shown in Fig. 10. The vibration caused by other stages cannot be avoided during the load-bearing process and the movement of the entire model, despite the fact that the largest deformation occurs in the non-bearing portion. The upper portion is comprised of plastic (detail of the shell), so it is easily deformed by external forces.

#### 4.2.4. Factor of safety

From the results of the Fig. 11, we can determine the most hazardous position, as well as the deformation and displacement caused by the load and the model. However, in addition to dangerous locations, different portions are susceptible to varying weights dispersed across the section, and each part has its own dangerous positions. Here, the simulation provides only the values of stress, displacement, deformation, and safety factor for the entire model, without identifying the model with the optimal structure (at points of excess strength and instability). To tackle this issue, we employ a topology optimization method.

#### 4.3. Topology optimization

The objective of this problem is to change the size of the part to increase its strength, evenly distribute the stress, and decrease its weight.

The optimization problem considers every detail before determining the optimal model structure. In addition to the most dangerous position on the model, it can be seen that the 2 arm joint is a component that bears a substantial load, and that the stress distribution throughout the entire section is unequal. Therefore, select the details of the joint 2 arm accomplished in the optimization problem, locating the right texture and form. And the same two arm joint details can be used to the remaining details in order to construct a complete arm model.

To apply the optimization problem, we first simulate the detailed static of the 2-arm joint using the force model, as illustrated in the Fig. 12 and Table 5.

The simulation results for the model's stress, displacement, deformation, and safety factor are provided below.  $\delta_{Max} = 2.776 + 06 \text{ N/m}^2$  is significantly less than the maximum permissible  $[\delta_{Max}] = 5.515e + 07 \text{ N/m}^2$  as determined by simulation. Consequently, the structure of

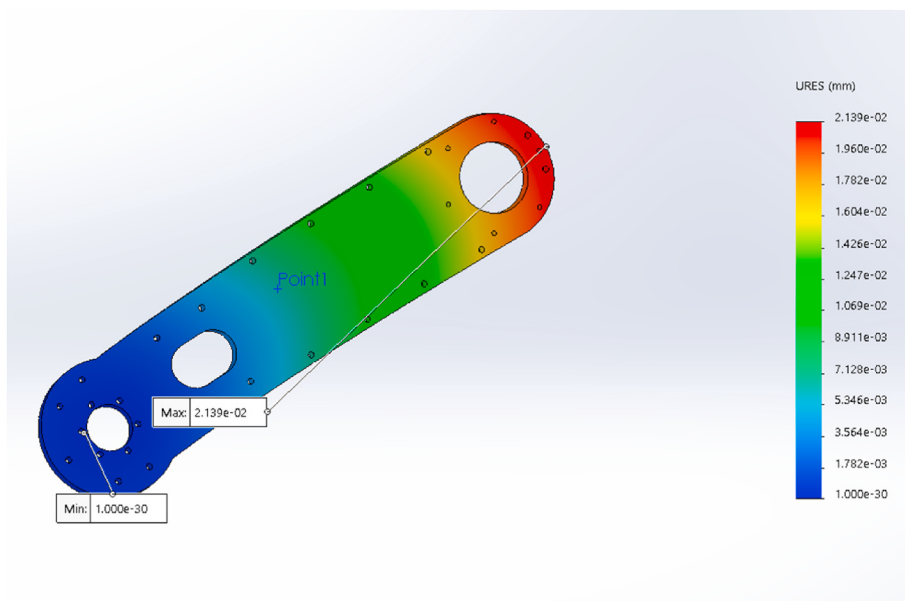


**Fig. 18.** Displacement from new structure.

the detail is sufficiently robust. Nonetheless, there are numerous regions where stress concentration is high and duplicated sites are robust. Without performing the optimization problem, the simulation result for joint 2arm is depicted in the picture below. The simulation results of stress, deformation, displacement, and safety factor of 2arm joint details are presented, accordingly, from left to right and from top to bottom as shown in the Fig. 13.

According to the results of the component's static simulation, there are numerous huge redundant places. To solve this problem, we will employ the topology algorithm with the objective of minimizing the part's volume.

Fig. 14 shown the outcomes of the optimization problem for a variety of scenarios with starting constraints. Including the recommended column for the optimal structure for the specifics.

Despite a negligible decrease in volume, the proposed model's dimensions changed and its stress rose. With the size variables  $k_1$ ,  $k_2$ , and  $k_3$ , we obtain the stress change graphs corresponding to figures a, b, and c when  $k_1$ ,  $k_2$ , and  $k_3$  vary, respectively as shown in Fig. 15.

The final result of solving optimization and topology problems is depicted in the Fig. 16. The mass of the original component is 0.567 kg, but after solving both problems, it is 0.55 kg. Important structural positions remain unchanged, so ensuring the structural technology.

Obtaining stress simulation results from new structure as shown in Fig. 17.

The most dangerous location on the component stays unaltered, but the maximum stress applied to the component is now closer to its strength limit. Consequently minimizing

Displacement form new structure as shown in Fig. 18. Similar to the stress, the displacement value has decreased from 0.059 mm to 0.0214 mm after solving the previous two problems.

## 5. Manufactural and experimental results

The robot arm's components are manufactured using CNC technology as shown in the Fig. 19. There are many parts are needed to be manufactured. In this paper, one example part will be shown. Firstly, it's modeled in Solidworks. Secondly, a toolpath (blue line) is generated and translate in a NC file. The NC file is imported to a CNC machine to produce the part.

Fig. 20 demonstrates the experimental results. The arm is capable of producing smooth movements, can move along a given trajectory, can

pick up an object from a set point and drop it to a given position in a short period of time. The robot arm can be controlled automatically, its movements are smooth, and it is capable of picking up and releasing objects according to a specified trajectory. A robotic arm that functions similarly to expensive products widely available on the market. However, the cost of manufacturing a robot arm is not excessively high, and the fabrication is not overly complex, making it ideal for small factories in developing nations such as Vietnam. The price of a commercially available AR3 robot is \$1823.66 USD, whereas the cost of proposed robot arm is around \$1000 USD.

## 6. Conclusion

This article presents a completed process for developing a robot arm from design, modeling, simulation, to manufacture. The experimental results show that the proposed robot arm capable of basic functioning. The main conclusions of this study are summarized as follows:

- (1) A robot arm with working dimension similar to a human arm is successfully manufactured.
- (2) The constructed cost is considerably lower cost than a commercial one.
- (3) The method could be used as a reference for develop a 6 DOF robot arm as well as evaluate the existing commercial product for optimal design.

## Credit author statement

**Tran Thanh Tung:** Writing, Software, Writing – original draft, Investigation. **Nguyen Van Tinh:** Manufacturing, Visualization. **Dinh Thi Phuong Thao:** Experiment, Manufacturing, Design, Software, Simulation. **Tran Vu Minh:** Conceptualization, Methodology, Supervision, Reviewing and Editing.

## Declaration of competing interest

The authors declare that they have no known competing financial interests or personal relationships that could have appeared to influence the work reported in this paper.

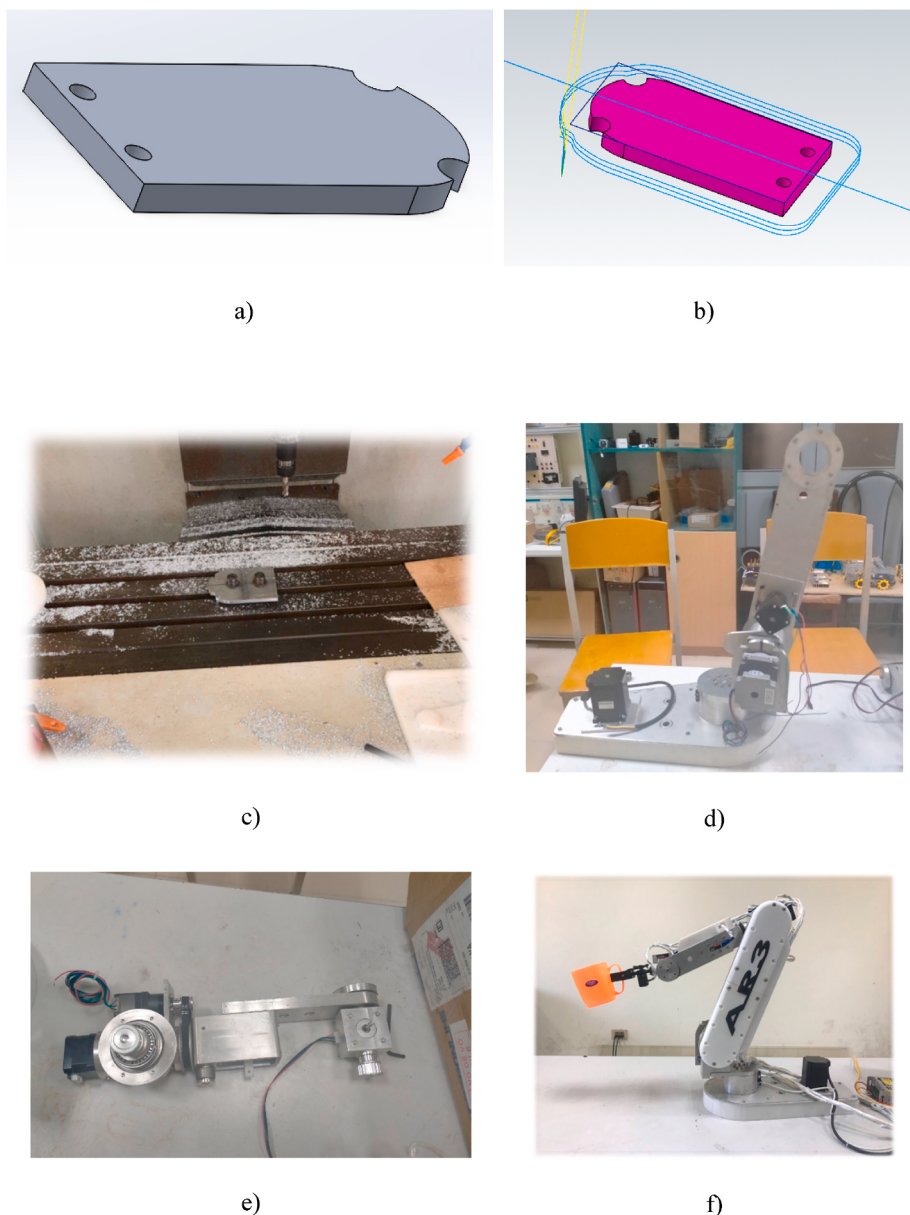


**Fig. 19.** Prototype's manufacturing process. a) part's model in Solidworks, b) Toolpath is generated, c) Cutting on CNC machine, d) Link 1 and 2 connections, e) Link 3 and 4 connections, f) completed prototype.

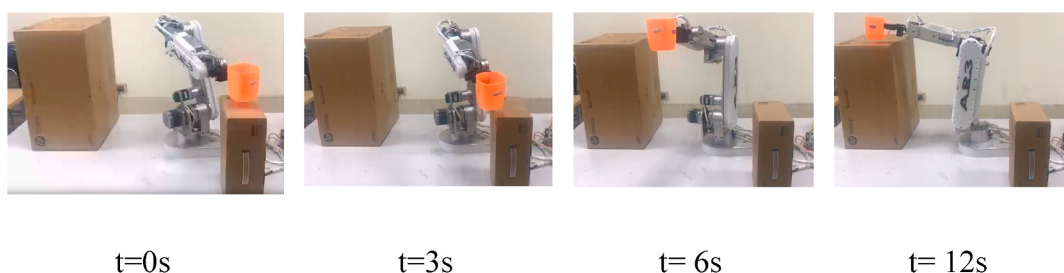


**Fig. 20.** Sequence of pick and place from experimental test.

## Data availability

Data will be made available on request.

## Acknowledgement

This research is funded by the Hanoi University of Science and Technology (HUST) under project number T2022-PC-028.

## Appendix A. Supplementary data

Supplementary data to this article can be found online at <https://doi.org/10.1016/j.rineng.2023.101049>.

## References

- [1] L. Birglen, T. Schlicht, A statistical review of industrial robotic grippers, *Robot. Comput. Integrated Manuf.* 49 (2018) 88–97.
- [2] Xiaolong Ke, Yongheng Yu, Kangsen Li, Tianyi Wang, Bo Zhong, Zhenzhong Wang, Lingbao Kong, Jiang Guo, Lei Huang, Mourad Idir, Chao Liu, Chunjin Wang, Review on robot-assisted polishing: status and future trends, *Robot. Comput. Integrated Manuf.* 80 (2023).
- [3] Achim Buerkle, William Eaton, Ali Al-Yacoub, Melanie Zimmer, Peter Kinnell, Michael Henshaw, Matthew Coombes, Wen-Hua Chen, Niels Lohse, Towards industrial robots as a service (IRaaS): flexibility, usability, safety and business models, *Robot. Comput. Integrated Manuf.* 81 (2023).
- [4] Michal Bartoš, Vladimír Bulej, Bohušek Martin, Ján Stanček, Vitalii Ivanov, Peter Macek, An overview of robot applications in automotive industry, *Transport. Res. Procedia* 55 (2021).
- [5] Mikkel Rath Pedersen, Lazaros Nalpantidis, Rasmus Skovgaard Andersen, Casper Schou, Bøgh Simon, Volker Krüger, Ole Madsen, Robot skills for manufacturing: from concept to industrial deployment, *Robot. Comput. Integrated Manuf.* 37 (2017).
- [6] C. Zheng, X. Qin, B. Eynard, J. Bai, J. Li, Y. Zhang, SME-oriented flexible design approach for robotic manufacturing systems, *J. Manuf. Syst.* 53 (2019) 62–74, <https://doi.org/10.1016/j.jmsy.2019.09.010>.
- [7] Mikkel Rath Pedersen, Lazaros Nalpantidis, Rasmus Skovgaard Andersen, Casper Schou, Bøgh Simon, Volker Krüger, Ole Madsen, Robot skills for manufacturing: from concept to industrial deployment, *Robot. Comput. Integrated Manuf.* 37 (2016) 282–291, <https://doi.org/10.1016/j.rcim.2015.04.002>.
- [8] A. Kapitonov, S. Lonshakov, V. Bulatov, B.K. Montazam, J. White, Robot-as-a-Service: from cloud to peering technologies, *Front. Robot. AI* 8 (2021) 1–7, <https://doi.org/10.3389/frobt.2021.560829>.
- [9] A. Billard, D. Kragic, Trends and challenges in robot manipulation, *Science.* (80-. ) (2019) 364, <https://doi.org/10.1126/science.aat8414>, 6446.
- [10] Bahareh Vaisi, A review of optimization models and applications in robotic manufacturing systems: industry 4.0 and beyond, *Decis. Anal. J.* 2 (2022).
- [11] Chien-Chiang Lee, Shuai Qin, Yaya Li, Does industrial robot application promote green technology innovation in the manufacturing industry? *Technol. Forecast. Soc. Change* 183 (2022).
- [12] Atieh Hanna, Simon Larsson, Per-Lage Götwall, Kristofer Bengtsson, Deliberative safety for industrial intelligent human–robot collaboration: regulatory challenges and solutions for taking the next step towards industry 4.0, *Robot. Comput. Integrated Manuf.* 78 (2022).
- [13] Mohd Javaid, Abid Haleem, Ravi Pratap Singh, Rajiv Suman, Substantial capabilities of robotics in enhancing industry 4.0 implementation, *Cognit.Robot.* 1 (2021).
- [14] Jorge Ribeiro, Rui Lima, Tiago Eckhardt, Sara Paiva, Robotic process automation and artificial intelligence in industry 4.0 – a literature review, *Proc. Comput. Sci.* 181 (2021).
- [15] Nafiu Abubakar Abdulrazaq, Lata Dhar Suman, Abdullaee Abba Tijjani, Auwalu Muhammad Abdullahi, Automated liquid filling system with a robotic arm conveyor for small scale industries, *Mater. Today Proc.* 49 (Part 8) (2022).
- [16] Lu Zhang, Tao Xie, Shaopeng He, Hao Liang, Shengjun Shi, Xiaobiao Shan, A simple linear driving actuator for robotic arm used in land-deep sea, *Mech. Syst. Signal Process.* 170 (2022).
- [17] Vikas Paradkar, Hifjur Raheman, K. Rahul, Development of a metering mechanism with serial robotic arm for handling paper pot seedlings in a vegetable transplanter, *Artif. Intell. Agric.* 5 (2021).
- [18] Rafal Siemasz, Krzysztof Tomczuk, Ziemowit Malecha, 3D printed robotic arm with elements of artificial intelligence, *Proc. Comput. Sci.* 176 (2020) 3741–3750.
- [19] Hiroaki Seki, Shota Nakayama, Kunio Uenishi, Tokuo Tsuji, Masatoshi Hikiz, Yutaka Makino, Akira Kakiuchi, Yoshikazu Kanda, Development of assistive robotic arm for power line maintenance, *Precis. Eng.* 67 (2021).
- [20] Aolei Yang, Yanling Chen, Wasif Naeem, Minrui Fei, Ling Chen, Humanoid motion planning of robotic arm based on human arm action feature and reinforcement learning, *Mechatronics* 78 (2021).
- [21] H. Toyama, H. Kawamoto, Y. Sankai, Development of cybernic robot arm to realize support action cooperated with hemiplegic person's arm 2019, in: 41st Annual International Conference of the IEEE Engineering in Medicine and Biology Society (EMBC), 2019, pp. 1645–1650.
- [22] N. García, J. Rosell, R. Suárez, Motion planning by demonstration with human-likeness evaluation for dual-arm robots, *IEEE Trans. Syst., Man, Cybernet.: Systems* 49 (11) (2019) 2298–2307.
- [23] B. Xie, J. Zhao, Y. Liu, Human-like motion planning for robotic arm system, in: 15th International Conference on Advanced Robotics (ICAR), 2011, pp. 88–93 (June).
- [24] Primož Bencák, Darko Hercog, Tone Lerher, Evaluating robot bin-picking performance based on Box and Blocks Test, *IFAC-PapersOnLine* 55 (10) (2022).
- [25] R. Shah, A.B. Pandey, Concept for automated sorting robotic arm, *Procedia Manuf.* 20 (2018).
- [26] Agathoklis A. Krimpenisa, Vasileios Papapaschosa, Evgenios Bontarenko, HydraX, a 3D printed robotic arm for hybrid manufacturing. Part I: custom design, manufacturing and assembly, *Procedia Manuf.* 51 (2020) 103–108.
- [27] M.Z. Silva, T. Brito, J.L. Lima, M.F. Silva, Industrial robotic arm in machining process aimed to 3D objects reconstruction, in: 2021 22nd IEEE International Conference on Industrial Technology (ICIT), 2021, pp. 1100–1105, <https://doi.org/10.1109/ICIT46573.2021.9453596>.
- [28] W. Ji, L. Wang, Industrial robotic machining: a review, *Int. J. Adv. Manuf. Technol.* 103 (1–4) (2019) 1239–1255.
- [29] Yu-Hsiang Chang, Chia-Hao Liang, Chao-Chieh Lan, An end-effector wrist module for the kinematically redundant manipulation of arm-type robots, *Mech. Mach. Theor.* 155 (2021).
- [30] P. Sun, Y. Li, Z. Wang, K. Chen, B. Chen, X. Zeng, J. Zhao, Y. Yue, Inverse displacement analysis of a novel hybrid humanoid robotic arm, *Mech. Mach. Theor.* 147 (2020).
- [31] X. Wang, D. Zhang, C. Zhao, H. Zhang, H. Yan, Singularity analysis and treatment for a 7R 6-DOF painting robot with non-spherical wrist, *Mech. Mach. Theor.* 126 (2018) 92–107.
- [32] Chenglong Yu, Zhiqi Li, Dapeng Yang, Hong Liu, A fast robotic arm gravity compensation updating approach for industrial application using sparse selection and reconstruction, *Robot. Autonom. Syst.* 149 (2022).
- [33] C. Urrea, J. Pascal, Design, simulation, comparison and evaluation of parameter identification methods for an industrial robot, *Comput. Electr. Eng.* 67 (2018) 791–806.
- [34] ANNIN ROBOTICS. <https://www.anninrobotics.com/>.